Naval Research Laboratory

Washington, DC 20375-5320

NRL/MR/5344--19-9896

An Approximate Bayesian Extended Target Tracking Algorithm

David F. Crouse

Surveillance Technology Branch
Radar Division

December 10, 2019

REPORT DOCUMENTATION PAGE

Form Approved
OMB No. 0704-0188

1. REPORT DATE *(DD-MM-YYYY)*
10-12-2019

2. REPORT TYPE
NRL Memorandum Report

3. DATES COVERED *(From - To)*

4. TITLE AND SUBTITLE

An Approximate Bayesian Extended Target Tracking Algorithm

5a. CONTRACT NUMBER

5b. GRANT NUMBER

5c. PROGRAM ELEMENT NUMBER

6. AUTHOR(S)

David F. Crouse

5d. PROJECT NUMBER
53-1J47-09

5e. TASK NUMBER

5f. WORK UNIT NUMBER
1J47

7. PERFORMING ORGANIZATION NAME(S) AND ADDRESS(ES)

Naval Research Laboratory
4555 Overlook Avenue, SW
Washington, DC 20375-5320

8. PERFORMING ORGANIZATION REPORT NUMBER

NRL/MR/5344--19-9896

9. SPONSORING / MONITORING AGENCY NAME(S) AND ADDRESS(ES)

Office of Naval Research
One Liberty Center
875 North Randolph Street, Suite 1425
Arlington, VA 22203

10. SPONSOR / MONITOR'S ACRONYM(S)

ONR

11. SPONSOR / MONITOR'S REPORT NUMBER(S)

12. DISTRIBUTION / AVAILABILITY STATEMENT

DISTRIBUTION STATEMENT A: Approved for public release; distribution is unlimited.

13. SUPPLEMENTARY NOTES

14. ABSTRACT

Extended target tracking treats clusters of detections from one or more targets as one large entity to be tracked. The simplest algorithms approximate the shape of the extended target using an ellipsoid. Modern algorithms for filtering measurements for extended target tracks are based on approximations to Bayes' theorem. This memo presents a new, simple approximation to the measurement-update step of an extended target-tracking filter as well as a heuristic for track initialization. Like previous work, the filter uses a Gaussian approximation for the center of the target ellipsoid and an inverse-Wishart distribution to represent the uncertainty in the shape of the ellipsoid.

15. SUBJECT TERMS

Extended target tracking, Group tracking, Cluster tracking, Bayesian estimation, Kalman filter

16. SECURITY CLASSIFICATION OF: a. REPORT	b. ABSTRACT	c. THIS PAGE	17. LIMITATION OF ABSTRACT	18. NUMBER OF PAGES	19a. NAME OF RESPONSIBLE PERSON
Unclassified Unlimited	Unclassified Unlimited	Unclassified Unlimited	Unclassified Unlimited	14	David F. Crouse
					19b. TELEPHONE NUMBER *(include area code)* (202) 404-8106

Standard Form 298 (Rev. 8-98)
Prescribed by ANSI Std. Z39.18

This page intentionally left blank.

An Approximate Bayesian Extended Target-Tracking Algorithm

David Frederic Crouse*

Abstract

Extended target tracking treats clusters of detections from one or more targets as one large entity to be tracked. The simplest algorithms approximate the shape of the extended target using an ellipsoid. Modern algorithms for filtering measurements for extended target tracks are based on approximations to Bayes' theorem. This memo presents a new, simple approximation to the measurement-update step of an extended target-tracking filter as well as a heuristic for track initialization. Like previous work, the filter uses a Gaussian approximation for the center of the target ellipsoid and an inverse-Wishart distribution to represent the uncertainty in the shape of the ellipsoid.

I. Introduction

EXTENDED target tracking, also known as "group tracking," "centroid group tracking," and "formation group tracking," is an approach to tracking large targets that produce multiple detections or for tracking multiple small targets that travel in a group and are simpler to track collectively than individually. Such algorithms were considered as an important part of the Strategic Defense Initiative's tracking system in the 1980s [11]. The algorithms are often broken into different categories as listed in [3, Ch. 6.9]:

1) Group tracking without individual tracks.
2) Group tracking with simplified individual tracks.
3) Individual tracking supplemented by group information.

This memo only considers the first type of extended target tracking.

Much of the work on extended target tracking prior to 2005 is summarized in the survey paper [25] and is covered in the monograph [12]. More recent work is covered in the survey [13] and end-to-end algorithms demonstrated on real data are described in [24], [14]. Extended target tracking was once again considered in a missile-tracking context in the conference paper (in Turkish) [21].

In 2005, Koch and Saul published a paper offering a rigorously Bayesian approach to estimating an extended target state represented as an ellipsoid [18]. The notion of representing a target in terms of ellipsoid parameters goes as far back as 1990 [7]. The algorithms prior to 2005 were somewhat more *ad-hoc* in their derivations. Koch and Saul's work is further developed in the 2008 journal article by Koch [17]. However, the algorithm is limited, because it requires the target state to take a particular restrictive format. One could not, for example, have a target state with a turn-rate component. The subsequent work of Feldmann, Fränken, and Koch in [9], [8] eliminates this restriction, but the derivation is an *ad-hoc* extension of Koch's work, rather than making clear approximations from an ideal Bayesian update.

The algorithm presented in this memo is a Bayesian derivation of an extended target-tracking update routine algorithm that has a form similar to that of Feldmann, Fränken, and Koch. However, approximations are made in clear positions. Simulations in Section VII provide an example where the algorithm of this work outperforms that of [9] and a related algorithm in [20].

Section II describes the probability distribution functions (PDFs) that will be used in the derivation of the filter and it lists a number of identities of the PDFs. Section III then discusses the definition of the target ellipsoid, which is consistent with previous models in the literature. The new Bayesian extended target-tracking algorithm is described in Section IV. An approach to initialize the filter is given in Section V. A simulation example is given in Section VII and the results are presented in Section VIII.

II. Preliminary Identities From the Literature

A. PDFs

The derivations utilize the multivariate normal distribution as well as the Wishart and inverse Wishart distributions. The $d-$dimensional multivariate normal PDF evaluated at $\mathbf{x}$ with mean $\hat{\boldsymbol{\mu}}$ and covariance matrix $\boldsymbol{\Sigma}$ is

$$\mathcal{N}_d\left\{\mathbf{x};\hat{\boldsymbol{\mu}},\boldsymbol{\Sigma}\right\}=\left|\boldsymbol{\Sigma}\right|^{-\frac{1}{2}}e^{-\frac{1}{2}(\mathbf{x}-\hat{\boldsymbol{\mu}})^T\boldsymbol{\Sigma}^{-1}(\mathbf{x}-\hat{\boldsymbol{\mu}})}. \tag{1}$$

*The author is employed by the Naval Research Laboratory, Attn: Code 5344, 4555 Overlook Ave., SW, Washington DC 20375. (e-mail: david.crouse@nrl.navy.mil)

Manuscript approved September 20, 2019.

The d-dimensional Wishart distribution [15, Ch. 3.2] with $n > d-1$ degrees of freedom and $(d \times d)$ dimensional positive definite symmetric scale matrix $\mathbf{V}$ is:

$$\mathcal{W}_d\left\{\mathbf{X}; n, \mathbf{V}\right\} = \frac{|\mathbf{X}|^{\frac{n-d-1}{2}}}{2^{\frac{np}{2}}\,|\mathbf{V}|^{\frac{n}{2}}\,\Gamma_d\left(\frac{n}{2}\right)}\operatorname{etr}\left\{-\frac{1}{2}\mathbf{V}^{-1}\mathbf{X}\right\} \tag{2}$$

where $\Gamma_d(x)$ is the multivariate gamma function given by

$$\Gamma_d(x) = \pi^{\frac{d(d-1)}{4}}\prod_{i=1}^{d}\Gamma\left(a - \frac{i-1}{2}\right). \tag{3}$$

The mean of the Wishart distribution is

$$\mathrm{E}\left\{\mathbf{X}\right\} = n\mathbf{V}. \tag{4}$$

Given N samples, $\mathbf{x}_1, \ldots, \mathbf{x}_N$ of a multivariate d-dimensional Gaussian distribution with mean $\boldsymbol{\mu}$ and covariance matrix $\boldsymbol{\Sigma}$, the sample mean $\bar{\mathbf{x}}$ and the sample scatter matrix (non-normalized sample covariance matrix) are given by

$$\bar{\mathbf{x}} = \frac{1}{N}\sum_{i=1}^{N}\mathbf{x}_i \qquad \bar{\mathbf{X}} = \sum_{i=1}^{N}\left(\mathbf{x}_i - \bar{\mathbf{x}}\right)\left(\mathbf{x}_i - \bar{\mathbf{x}}\right)^T. \tag{5}$$

As noted in [6, Ch. 5.5], $\bar{\mathbf{x}}$ and $\bar{\mathbf{X}}$ are independent. Additionally, $\bar{\mathbf{x}} \sim \mathcal{N}\left\{\boldsymbol{\mu}, \boldsymbol{\Sigma}\right\}$ and $\bar{\mathbf{X}} \sim \mathcal{W}_d\left\{N-1, \boldsymbol{\Sigma}\right\}$. The notation $\sim$ here means "is distributed as" and the PDFs are shown with the parameters but omitting the argument. On the other hand, if $\mathbf{x}_i$ are samples of a multivariate d-dimensional zero-mean Gaussian distribution with covariance matrix $\boldsymbol{\Sigma}$, then it can be shown that

$$\sum_{i=1}^{N}\mathbf{x}_i\mathbf{x}_i^T \sim \mathcal{W}_d\left\{N, \boldsymbol{\Sigma}\right\}. \tag{6}$$

That is, knowing the mean of the underling normal distribution leads to having one more degree of freedom in the Wishart distribution for the scatter matrix.

Generation of Wishart random variables by summing normal outer products as in (6) is inefficient for large N. Also, one cannot generate Wishart random variables with non-integer degrees of freedom using such a technique. The Bartlett decomposition is a technique for generating Wishart random variables that scales in complexity with d^2, not N. It is described in [19] and in [16], with the derivation done in such a manner that it is clear that it works for non-integer degrees of freedom.

If $\mathbf{X} \sim \mathcal{W}_d\left\{n, \mathbf{V}\right\}$, then $\mathbf{X}^{-1} \sim \mathcal{IW}_d\left\{n, \mathbf{V}^{-1}\right\}$, where $\mathcal{IW}_d$ refers to the inverse Wishart (inverted Wishart) distribution [15, Ch. 3.4]. The d-dimensional inverse Wishart distribution with $n > d-1$ degrees of freedom and $(d \times d)$ positive-definite, symmetric precision matrix $\boldsymbol{\Psi}$ is

$$\mathcal{IW}_d\left\{\mathbf{X}; n, \boldsymbol{\Psi}\right\} = \frac{|\boldsymbol{\Psi}|^{\frac{n}{2}}}{2^{\frac{np}{2}}\,|\mathbf{X}|^{\frac{n+p+1}{2}}\,\Gamma_p\left(\frac{n}{2}\right)}\operatorname{etr}\left\{-\frac{1}{2}\boldsymbol{\Psi}\mathbf{X}^{-1}\right\}. \tag{7}$$

The mean of the inverse Wishart distribution is

$$\mathrm{E}\left\{\mathbf{X}\right\} = \frac{\boldsymbol{\Psi}}{n-p-1}. \tag{8}$$

A definition of the covariance of an inverse-Wishart distribution is $(\alpha > 2)$

$$\mathrm{E}\left\{\left(\mathbf{X}_k - \hat{\mathbf{X}}\right)\left(\mathbf{X}_k - \hat{\mathbf{X}}\right)^T\right\} = \frac{\alpha\operatorname{trace}\left\{\hat{\mathbf{X}}\right\}\hat{\mathbf{X}} + (\alpha+2)\hat{\mathbf{X}}^2}{(\alpha+1)(\alpha-2)} \tag{9}$$

$$\alpha \triangleq n - d - 1. \tag{10}$$

Note that the covariance of the inverse Wishart distribution diverges as $\alpha \to 2$.

The inverse Wishart distribution is often used as a conjugate-prior PDF for estimating the covariance matrix of a multivariate normal distribution given samples and the Wishart distribution is often used as a conjugate-prior PDF for a precision matrix (an inverse covariance matrix) of a multivariate normal distribution.

B. PDF Relations

Given an inverse-Wishart prior, if $\boldsymbol{\mu}$ is a constant (i.e. Bayesian update with a normal likelihood), then it can be shown that

$$\mathcal{N}\left\{\boldsymbol{\mu}; \hat{\boldsymbol{\mu}}, \frac{1}{\kappa}\mathbf{P}\right\}\mathcal{IW}_d\left\{\mathbf{P}; \nu, \mathbf{V}\right\} \propto \mathcal{IW}_d\left\{\mathbf{P}; \nu+1, \kappa\left(\boldsymbol{\mu} - \hat{\boldsymbol{\mu}}\right)\left(\boldsymbol{\mu} - \hat{\boldsymbol{\mu}}\right)^T + \mathbf{V}\right\} \tag{11}$$

where $\propto$ means "proportional to" (discarding normalizing constants). This means that the inverse Wishart distribution is *conjugate prior* to the normal distribution with a known mean. Put differently, given a prior of $\mathcal{IW}_d\{\mathbf{P};\nu,\mathbf{V}\}$ and a measurement with known mean $\hat{\boldsymbol{\mu}}$ and unknown covariance matrix scaled by $\frac{1}{\kappa}$, the posterior distribution is Inverse-Wishart with parameters

$$\nu_{\text{posterior}} = \nu + 1 \qquad \mathbf{V}_{\text{posterior}} = \kappa\left(\boldsymbol{\mu}-\hat{\boldsymbol{\mu}}\right)\left(\boldsymbol{\mu}-\hat{\boldsymbol{\mu}}\right)^T + \mathbf{V}. \tag{12}$$

An estimate for the unknown scaled covariance matrix is the expected value of the inverse-Wishart distribution from (4):

$$\mathrm{E}\{\mathbf{P}\} = \frac{\mathbf{V}}{\nu - d - 1}. \tag{13}$$

The product of N normal PDFs can be expressed in terms of a Wishart distribution as [8, Eq. 2.22]

$$\prod_{i=1}^{n_k}\mathcal{N}_d\{\mathbf{x}_i;\hat{\boldsymbol{\mu}},\boldsymbol{\Sigma}\} = |2\pi\boldsymbol{\Sigma}|^{-\frac{n_k}{2}}\,e^{-\frac{1}{2}\sum_{i=1}^{n_k}(\mathbf{x}_i-\hat{\boldsymbol{\mu}})^T\boldsymbol{\Sigma}^{-1}(\mathbf{x}_i-\hat{\boldsymbol{\mu}})} = \frac{1}{c_d(\bar{\mathbf{X}},n)}\mathcal{N}_d\left\{\bar{\mathbf{x}};\hat{\boldsymbol{\mu}},\frac{1}{n}\boldsymbol{\Sigma}\right\}\mathcal{W}_d\left\{\bar{\mathbf{X}};n-1,\boldsymbol{\Sigma}\right\} \tag{14}$$

where, when treating as likelihoods ($\mathbf{x}_i$ are measurements), c_d is the constant:

$$c_d(\bar{\mathbf{X}},n_k)^{-1} = \Gamma_d\left(\frac{n_k-1}{2}\right)\pi^{-\frac{d}{2}(n_k-1)}n_k^{-\frac{1}{2}d}\left|\bar{\mathbf{X}}\right|^{-\frac{1}{2}(n_k-d-2)}. \tag{15}$$

The transformation comes from rewriting the argument of the exponential in terms of matrix traces and rearranging the terms.

The product of the Wishart and inverse Wishart distributions is [17, Appen. B.6]

$$\mathcal{W}_d\{\mathbf{Z};n_1,a\mathbf{X}\}\,\mathcal{IW}_d\{\mathbf{X};n_2,\boldsymbol{\Psi}\} = \mathcal{IW}_d\left\{\mathbf{X};n_1+n_2,\frac{\mathbf{Z}}{a}+\boldsymbol{\Psi}\right\} \tag{16}$$

$$c_d^1 = \frac{a^{-\frac{1}{2}d(d+1)}\Gamma_d\left(\frac{n_1+n_2}{2}\right)}{\left|\frac{\mathbf{Z}}{a}\right|^{\frac{n_2+d+1}{2}}\left|\boldsymbol{\Psi}\right|^{\frac{n_1}{2}}\Gamma_d\left(\frac{n_1}{2}\right)\Gamma_d\left(\frac{n_2}{2}\right)}. \tag{17}$$

The inverse-Wishart distribution is thus conjugate prior to the Wishart distribution when estimating n_2 and $\boldsymbol{\Psi}$.

The final identity that shall be used relates to the product of two normal distributions of forms arising in Kalman filtering. Specifically [8, Append. B.4]

$$\mathcal{N}_d\{\mathbf{z};\mathbf{H}\mathbf{x},\mathbf{R}\}\,\mathcal{N}_p\{\mathbf{x};\boldsymbol{\mu},\mathbf{P}\} = \mathcal{N}_d\{\mathbf{z};\mathbf{H}\boldsymbol{\mu},\mathbf{S}\}\,\mathcal{N}_p\left\{\mathbf{x};\boldsymbol{\mu}_{\text{post}},\mathbf{P}_{\text{post}}\right\} \tag{18}$$

with

$$\boldsymbol{\mu}_{\text{pos}} = \boldsymbol{\mu} + \mathbf{K}\left(\mathbf{z}-\mathbf{H}\boldsymbol{\mu}\right) \tag{19}$$

$$\mathbf{P}_{\text{post}} = -\mathbf{K}\mathbf{S}\mathbf{K}^T = \left(\mathbf{I}-\mathbf{K}\mathbf{H}\right)\mathbf{P}\left(\mathbf{I}-\mathbf{K}\mathbf{H}\right)^T + \mathbf{K}\mathbf{R}\mathbf{K}^T \tag{20}$$

$$\mathbf{S} = \mathbf{H}\mathbf{P}\mathbf{H}^T + \mathbf{R} \tag{21}$$

$$\mathbf{K} = \mathbf{P}\mathbf{H}^T\mathbf{S}^{-1}. \tag{22}$$

These are the identities making up the Kalman filter. The expression in (20) is the Joseph form of the covariance update [1, Ch. 5.2.3]. A derivation of the product is given in [8, Appendix B.4]. However, it can be obtained in a number of ways. Note that the dimensionalities d and p can be different. $\mathbf{H}$ is a $(d \times p)$-dimensional matrix.

The identities of this section shall play a role in the derivation of a recursive Bayesian extended target-tracking algorithm.

III. The Definition of the Ellipsoid

The ellipsoidal approximation for the target extent is developed here in a manner similar to [10], [8]. The shape of an extended target is approximated as an ellipse in 2D or an ellipsoids in 3D. It is assumed that detections are uniformly distributed over the ellipsoidal region. An ellipse or ellipsoid is defined to be the set of all points $\mathbf{p}$ such that

$$\left(\mathbf{p}-\mathbf{p}_0\right)\boldsymbol{\Sigma}^{-1}\left(\mathbf{p}-\mathbf{p}_0\right) \leq 1 \tag{23}$$

where $\mathbf{p}_0$ is the center of the ellipsoid and positive-definite matrix $\boldsymbol{\Sigma}$ defines the shape of the ellipsoid.

It is known [2, Ch. 2.3.2] that the volume of a d-dimensional ellipsoid defined as above is

$$V_d = \frac{|\boldsymbol{\Sigma}|^{\frac{1}{2}}\pi^{\frac{d}{2}}}{\Gamma(\frac{d}{2}+1)}. \tag{24}$$

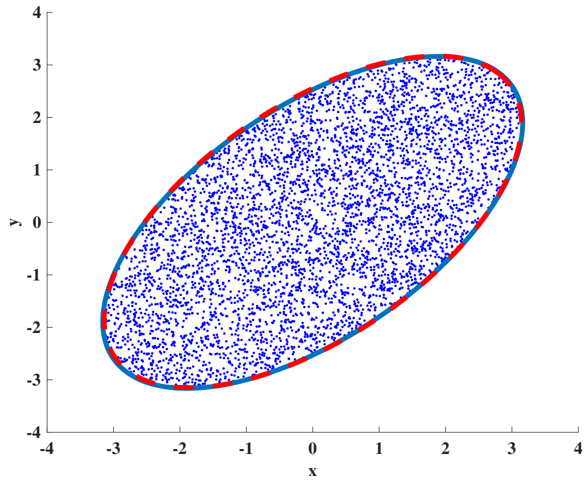

Fig. 1. 10^4 uniform random samples from a 2D ellipse. The blue line is the ellipse boundary; the dashed red line is the normal approximation to the boundary using the sample mean and covariance with $z_d = 1/4$.

Consequently, the uniform distribution over a d dimensional ellipsoid is:

$$\mathcal{U}_d \left\{\mathbf{p}; \boldsymbol{\Sigma}\right\} = \begin{cases} \frac{\Gamma(\frac{n}{2}+1)}{\left|\boldsymbol{\Sigma}\right|^{\frac{1}{2}} \pi^{\frac{d}{2}}} & \text{If } \left(\mathbf{p}-\mathbf{p}_0\right)^T \boldsymbol{\Sigma} \left(\mathbf{p}-\mathbf{p}_0\right) \leq 1 \\ 0 & \text{Otherwise} \end{cases}. \tag{25}$$

As derived in Appendix A, the covariance matrix of the uniform distribution over a d-dimensional ellipsoid is

$$\mathrm{E}\left\{\left(\mathbf{p}-\mathbf{p}_0\right)\left(\mathbf{p}-\mathbf{p}_0\right)^T\right\} = \frac{1}{d+2}\boldsymbol{\Sigma} \tag{26}$$

Despite the appeal of modeling detections from an extended target as coming from a uniformly distributed ellipsoid, Gaussian approximations tend to be more amenable to the derivation of recursive estimation algorithms. Consequently, ignoring measurement noise, we approximate the measurement from a target as

$$\mathbf{p} \sim \mathcal{N}\left\{\mathbf{p}_0, z_d \boldsymbol{\Sigma}\right\} \tag{27}$$

with

$$z_d = \frac{1}{d+2}. \tag{28}$$

The z_d scaling makes the second moment of the normal distribution match that of the uniform distribution. This type of moment matching was first introduced in [10].

To get an idea of the validity of the normal approximation in an ideal case, Fig. 1 plots 10^4 random samples from a 2D uniform ellipse distribution. The function `randPointInEllipsoid` in the Tracker Component Library (TCL) [5], [26], which implements the algorithm of [23, Sec. 3.1.3], was used to generate the uniformly distributed points.. The ellipsoid center was set to $\mathbf{p}_0\mathbf{0}$ and the spread term is

$$\boldsymbol{\Sigma} = \begin{bmatrix} 10 & 6 \\ 6 & 10 \end{bmatrix}. \tag{29}$$

The normal approximation plots the ellipse with

$$\left(\mathbf{p}-\hat{\mathbf{p}}\right)\left(\frac{1}{z_d}\mathbf{P}\right)^{-1}\left(\mathbf{p}-\hat{\mathbf{p}}\right) \leq 1 \tag{30}$$

where $\hat{\mathbf{p}}$ and $\mathbf{P}$ are the sample mean and the sample covariance matrix. The dashed red line in Fig. 1 is the normal approximation to the shape and the blue line is the actual outer extent of the ellipsoid (plotted using `drawEllipse` in the TCL). It can be seen that the fit of the normal approximation to the uniform samples is good.

IV. A Bayesian Derivation

Consistent with Section III, the extended target is modeled approximately as an ellipsoidal region in position. In this section, an approximate Bayesian method for updating the target position and extent information is derived. Only linear measurements are considered. At time k, one estimates the $(d_x \times 1)$ state vector $\mathbf{x}_k$. The $(d_z \times d_x)$ linear measurement matrix $\mathbf{H}$ extracts the position components of the target state. For example, for a state consisting of position and velocity in 3D space consisting of $[x, y, z, \dot{x}, \dot{y}, \dot{z}]^T$, one would use

$$\mathbf{H} = \begin{bmatrix} 1 & 0 & 0 & 0 & 0 & 0 \\ 0 & 1 & 0 & 0 & 0 & 0 \\ 0 & 0 & 1 & 0 & 0 & 0 \end{bmatrix}. \tag{31}$$

Given the center of the ellipsoid, $\mathbf{H}\mathbf{x}_k$, the shape is modeled as the region defined by a matrix $\mathbf{X}_k$ such that a point $\mathbf{p}$ is within the target extent if

$$(\mathbf{p} - \mathbf{H}\mathbf{x}_k)^T \mathbf{X}_k^{-1} (\mathbf{p} - \mathbf{H}\mathbf{x}_k) \leq 1. \tag{32}$$

However, this definition does not lend itself to a convenient formulation of the measurement-update equation. Consequently, the target extent is modeled as a modification of the measurement covariance, with a scale parameter z_d chosen so that the expected value of this covariance matrix equals the covariance matrix of the uniform distribution. This model is consistent with the extent representation of (30). The distribution of the ith measurement conditioned on the state $\mathbf{x}_k$ and the target-extent parameter $\mathbf{X}_k$ is thus modeled as:

$$p(\mathbf{z}_i|\mathbf{x}_k, \mathbf{X}_k) = \mathcal{N}\{\mathbf{z}_i; \mathbf{H}\mathbf{x}_k, z_d\mathbf{X}_k + \mathbf{R}_k\} \tag{33}$$

where $\mathbf{R}_k$ is a covariance matrix for measurement noise due to receiver noise and interference. This model is the same as (27) but with the additional of the measurement noise parameter and is the model used in [9], [8]. Note that while no real measurements will be given in Cartesian coordinates, unbiased measurement-conversion algorithms, such as the cubature methods mentioned in [4] can be used for unbiased measurement conversion. In the simulations here, the `pol2CartCubature` function in the TCL is used.

Measurements are assumed to be independent and no model is given for the number of measurements at a particular time from a target (i.e. assume a uniform [constant, uninformative] prior). The PDF of n_k measurements, with $\mathbf{Z}^k = \{z_1, \ldots, \mathbf{z}_{n_k}\}$ is thus:

$$p\left(\mathbf{Z}^k \middle| \mathbf{x}_k, \mathbf{X}_k, n_k\right) = \prod_{i=1}^{n_k} \mathcal{N}\{\mathbf{z}_i; \mathbf{H}\mathbf{x}_k, z_d\mathbf{X}_k + \mathbf{R}_k\} \tag{34}$$

$$= \frac{1}{c_d(\bar{\mathbf{Z}}, n)} \mathcal{N}_d\left\{\bar{\mathbf{z}}; \mathbf{H}\mathbf{x}_k, \frac{1}{n_k}(z_d\mathbf{X}_k + \mathbf{R}_k)\right\} \mathcal{W}_d\{\bar{\mathbf{Z}}; n_k - 1, z_d\mathbf{X}_k + \mathbf{R}_k\} \tag{35}$$

where the identity in (14) was used and where

$$\bar{\mathbf{z}} = \frac{1}{n_k}\sum_{i=1}^{n_k} \mathbf{z}_i \qquad \bar{\mathbf{Z}} = (\bar{\mathbf{z}} - \mathbf{z}_i)(\bar{\mathbf{z}} - \mathbf{z}_i)^T. \tag{36}$$

This is a linear model:

$$\mathbf{z}_i^k = \mathbf{H}\mathbf{x}_k + \mathbf{v}_k \tag{37}$$

where $\mathbf{v}_k$ is zero-mean Gaussian with covariance matrix $z_d\mathbf{X}_k + \mathbf{R}_k$.

Equation (33) is the measurement likelihood. The prior target state at time k, which includes information through time $k-1$, is taken to be a Gaussian distribution with mean $\hat{\mathbf{x}}_{k|k-1}$. The distribution of the target-extent variable $\mathbf{X}_k$ is taken to be an inverse-Wishart distribution with $\nu - k|k-1$ degrees of freedom and scale matrix $\tilde{\mathbf{X}}_{k|k-1}$. This means that the joint prior distribution is a term related to the center of the ellipsoid and a term related to the extent of the ellipsoid:

$$p(\mathbf{x}_k, \mathbf{X}_k) = p(\mathbf{x}_k|\mathbf{X}_k)\, p(\mathbf{X}_k) \tag{38}$$

$$= \mathcal{N}\left\{\mathbf{x}_k; \hat{\mathbf{x}}_{k|k-1}, \mathbf{P}_{k|k-1}\right\} \mathcal{IW}_d\left\{\mathbf{X}_k; \nu_{k|k-1}, \tilde{\mathbf{X}}_{k|k-1}\right\}. \tag{39}$$

Applying Bayes' rule to update the prior distribution given n_k measurements, one has (omitting the normalizing constants):

$$p\left(\mathbf{x}_k, \mathbf{X}_k \middle| \mathbf{Z}^k, n_k\right) \propto p\left(\mathbf{Z}^k \middle| \mathbf{x}_k, \mathbf{X}_k, n_k\right) p(\mathbf{x}_k, \mathbf{X}_k, n_k) \tag{40}$$

$$\propto \mathcal{N}_d\left\{\bar{\mathbf{z}}; \mathbf{H}\mathbf{x}_k, \frac{1}{n_k}(z_d\mathbf{X}_k + \mathbf{R}_k)\right\} \mathcal{N}\left\{\mathbf{x}_k; \hat{\mathbf{x}}_{k|k-1}, \mathbf{P}_{k|k-1}\right\} \mathcal{W}_d\{\bar{\mathbf{Z}}; n_k - 1, z_d\mathbf{X}_k + \mathbf{R}_k\} \mathcal{IW}_d\left\{\mathbf{X}_k; \nu_{k|k-1}, \tilde{\mathbf{X}}_{k|k-1}\right\}. \tag{41}$$

A. *Approximation for the Ellipsoid-Center Update*

The two normal distributions in (41) can be combined as in (18) to get:

$$p\left(\mathbf{x}_k, \mathbf{X}_k \middle| \mathbf{Z}^k, n_k\right) \propto p\left(\mathbf{Z}^k \middle| \mathbf{x}_k, \mathbf{X}_k, n_k\right) p(\mathbf{x}_k, \mathbf{X}_k, n_k) \tag{42}$$

$$\propto \mathcal{N}_d\left\{\bar{\mathbf{z}}; \mathbf{H}\hat{\mathbf{x}}_{k|k-1}, \mathbf{S}_k\right\} \mathcal{N}\left\{\mathbf{x}_k; \hat{\mathbf{x}}_{k|k}, \mathbf{P}_{k|k}\right\} \mathcal{W}_d\{\bar{\mathbf{Z}}; n_k - 1, z_d\mathbf{X}_k + \mathbf{R}_k\} \mathcal{IW}_d\left\{\mathbf{X}_k; \nu_{k|k-1}, \tilde{\mathbf{X}}_{k|k-1}\right\} \tag{43}$$

where

$$\begin{aligned}\tilde{\mathbf{R}}_k =&\frac{1}{n_k}\left(z_d\mathbf{X}_k+\mathbf{R}_k\right)\approx\frac{1}{n_k}\left(z_d\frac{\tilde{\mathbf{X}}_{k|k-1}}{\nu_{k|k-1}-d-1}+\mathbf{R}_k\right) && (44)\\
\mathbf{S}_k =&\tilde{\mathbf{R}}_k+\mathbf{H}\mathbf{P}_{k|k-1}\mathbf{H}^T && (45)\\
\mathbf{K}_k =&\mathbf{P}_{k|k-1}\mathbf{H}^T\mathbf{S}_k^{-1} && (46)\\
\hat{\mathbf{x}}_{k|k} =&\hat{\mathbf{x}}_{k|k-1}+\mathbf{K}_k\left(\bar{\mathbf{z}}-\mathbf{H}\hat{\mathbf{x}}_{k|k-1}\right) && (47)\\
\mathbf{P}_{k|k} =&\left(\mathbf{I}-\mathbf{K}_k\mathbf{H}\right)\mathbf{P}_{k|k-1}\left(\mathbf{I}-\mathbf{K}_k\mathbf{H}\right)^T+\frac{1}{n_k}\mathbf{K}_k\left(z_d\mathbf{X}_k+\mathbf{R}_k\right)\mathbf{K}_k^T. && (48)\end{aligned}$$

The approximation for $\tilde{\mathbf{R}}_k$ replaces $\mathbf{X}_k$ with its expected value in (44). This approximation decouples the equations and allows for a simple Kalman-filer update of the ellipsoid center.

B. Approximation for the Ellipsoid-Shape Update

To derive the update for the ellipsoid-shape parameters, we consider the case assuming that the target is large compared to the accuracy of the sensor. Assuming that $z_d\frac{\tilde{\mathbf{X}}_{k|k-1}}{\nu_{k|k-1}-d-1}\gg\mathbf{R}_k$, one can use the approximation that $\mathbf{R}_k\approx\mathbf{0}$.

$$p\left(\mathbf{x}_k,\mathbf{X}_k\left|\mathbf{Z}^k,n_k\right.\right)\propto\mathcal{N}_d\left\{\bar{\mathbf{z}}_k;\mathbf{H}\hat{\mathbf{x}}_{k|k-1},\mathbf{S}_k\right\}\mathcal{N}\left\{\mathbf{x}_k;\hat{\mathbf{x}}_{k|k},\mathbf{P}_{k|k}\right\}\mathcal{W}_d\left\{\bar{\mathbf{X}};n_k-1,z_d\mathbf{X}_k\right\}\mathcal{IW}_d\left\{\mathbf{X}_k;\nu_{k|k-1},\tilde{\mathbf{X}}_{k|k-1}\right\} \quad (49)$$

$$=\mathcal{N}_d\left\{\bar{\mathbf{z}}_k;\mathbf{H}\hat{\mathbf{x}}_{k|k-1},\mathbf{S}_k\right\}\mathcal{N}\left\{\mathbf{x}_k;\hat{\mathbf{x}}_{k|k},\mathbf{P}_{k|k}\right\}\mathcal{IW}\left\{\mathbf{X}_k;\nu_{k|k-1}+n_k-1,\frac{1}{z_d}\bar{\mathbf{Z}}_k+\tilde{\mathbf{X}}_{k|k-1}\right\} \quad (50)$$

$$=\mathcal{N}_d\left\{\bar{\mathbf{z}}_k;\mathbf{H}\hat{\mathbf{x}}_{k|k-1},\frac{z_d}{n_k}\mathbf{X}_k+\mathbf{H}\mathbf{P}_{k|k-1}\mathbf{H}^T\right\}\mathcal{N}\left\{\mathbf{x}_k;\hat{\mathbf{x}}_{k|k},\mathbf{P}_{k|k}\right\}\mathcal{IW}\left\{\mathbf{X}_k;\nu_{k|k-1}+n_k-1,\frac{1}{z_d}\bar{\mathbf{Z}}_k+\tilde{\mathbf{X}}_{k|k-1}\right\} \quad (51)$$

where the product identity for the Wishart and inverse-Wsihart PDFs of (16) is used.

To decouple the equations, approximate $\mathbf{x}_k=\hat{\mathbf{x}}_{k|k}$. Additionally, neglect the uncertainty in the center location of the ellipsoid using $\mathbf{P}_{k|k-1}\approx\mathbf{0}$. These substitutions put the equations in a form that can be simplified using (11)

$$\begin{aligned}&\mathcal{N}_d\left\{\bar{\mathbf{z}}_k;\mathbf{H}\hat{\mathbf{x}}_{k|k-1},\frac{z_d}{n_k}\mathbf{X}_k\right\}\mathcal{IW}\left\{\mathbf{X}_k;\nu_{k|k-1}+n_k-1,\frac{1}{z_d}\bar{\mathbf{Z}}_k+\tilde{\mathbf{X}}_{k|k-1}\right\}\propto\\
&\mathcal{IW}_d\left\{\mathbf{X}_k;\upsilon_{k|k-1}+n_k,\frac{n_k}{z_d}\left(\bar{\mathbf{z}}_k-\mathbf{H}\hat{\mathbf{x}}_{k|k}\right)\left(\bar{\mathbf{z}}_k-\mathbf{H}\hat{\mathbf{x}}_{k|k}\right)^T+\frac{1}{z_d}\bar{\mathbf{Z}}_k+\tilde{\mathbf{X}}_{k|k-1}\right\}. && (52)\end{aligned}$$

Consequently, the update is

$$\begin{aligned}\nu_{k|k} =&\nu_{k|k-1}+n_k && (53)\\
\tilde{\mathbf{X}}_{k|k} =&\tilde{\mathbf{X}}_{k|k-1}+\frac{1}{z_d}\bar{\mathbf{Z}}_k+\frac{n_k}{z_d}\left(\bar{\mathbf{z}}_k-\mathbf{H}\hat{\mathbf{x}}_{k|k}\right)\left(\bar{\mathbf{z}}_k-\mathbf{H}\hat{\mathbf{x}}_{k|k}\right)^T. && (54)\end{aligned}$$

An alternative approach to obtaining a simple update formula for the target extent could be to replace $\mathbf{x}_k$ in the first term of (41) with $\hat{\mathbf{x}}_{k|k-1}$ as this decouples the estimation of the ellipsoid-shape parameters from those for its center and again neglect $\mathbf{R}_k=\mathbf{0}$. This leads to the update equations:

$$\begin{aligned}\tilde{\mathbf{X}}_{k|k} =&\tilde{\mathbf{X}}_{k|k-1}+\frac{1}{z_d}\bar{\mathbf{Z}} && (55)\\
\nu_{k|k} =&\nu_{k|k-1}+n_k-1. && (56)\end{aligned}$$

However, it quickly becomes clear that this approximation to $\tilde{\mathbf{X}}_{k|k}$ is only meaningful if $n_k>1$. If $n_k=1$, then $\tilde{\mathbf{X}}_{k|k}=\tilde{\mathbf{X}}_{k|k-1}$ and $\nu_{k|k}=\nu_{k|k-1}$, which means that the measurement has no effect. Consequently, this simpler approximation is undesirable.

C. State Propagation

Given an approximation for a recursive measurement update, we need to propagate the ellipsoid center and extent forward in time. The measurement update puts the PDF into the same decoupled form as the assumed prior PDF:

$$p\left(\mathbf{x}_k,\mathbf{X}_k|\mathbf{Z}^k,n_k\right)=\mathcal{N}\left\{\mathbf{x}_k;\hat{\mathbf{x}}_{k|k},\mathbf{P}_{k|k}\right\}\mathcal{IW}_d\left\{\mathbf{X}_k;\nu_{k|k},\tilde{\mathbf{X}}_{k|k}\right\}. \quad (57)$$

The predicted ellipsoid-center parameters, $\hat{\mathbf{x}}_{k+1|k}$ and $\mathbf{P}_{k+1|k}$ can be obtained in the same manner as any point tracker (e.g. discrete or continuous-time Kalman-like propagation methods), because they are decoupled from the target-extent parameters.

To determine how to propagate the shape parameter, as in [9], [8], we look at a scalar measure of the accuracy of the inverse Wishart distribution, the mean-squared error (MSE):

$$e_{k|k} = \operatorname{trace}\left\{\mathrm{E}\left\{\left(\mathbf{X}_k - \hat{\mathbf{X}}_{k|k}\right)\left(\mathbf{X}_k - \hat{\mathbf{X}}_{k|k}\right)^T\right\}\right\} \tag{58}$$

where for $\alpha_{k|k} > 2$:

$$\hat{\mathbf{X}}_{k|k} = \frac{\tilde{\mathbf{X}}_k}{\alpha_{k|k}} \qquad \alpha_{k|k} = \nu_{k|k} - d - 1. \tag{59}$$

The MSE value $e_{k|k}$ is the trace of the covariance previously provided for the inverse-Wishart distribution. This simplifies to

$$e_{k|k} = \frac{\alpha_{k|k}\left(\alpha_{k|k}\operatorname{trace}\left\{\hat{\mathbf{X}}_{k|k}\right\}\right)^2 + \left(\alpha_{k|k}+2\right)\operatorname{trace}\left\{\mathbf{X}_{k|k}^2\right\}}{(\alpha_{k|k}+1)(\alpha_{k|k}-2)} \tag{60}$$

and it can be seen that $e_{k|k}$ diverges as $\alpha_{k|k} \to 2$.

We adopt the heuristics introduced in [8], [9]. The heuristics for propagating the target extent leave the expected value of the shape unchanged, but decrease ν so as to increase the uncertainty in the state. Given $\nu_{k+1|k}$ and $\nu_{k|k}$, $\tilde{\mathbf{X}}_{k+1|k}$ is obtained by scaling $\tilde{\mathbf{X}}_{k|k}$ to ensure the expected value does not change

$$\tilde{\mathbf{X}}_{k+1|k} = \frac{\alpha_{k+1|k}}{\alpha_{k|k}}\tilde{\mathbf{X}}_{k|k}. \tag{61}$$

An exponential propagation heuristic for a timespan of T given in [8], [9] is

$$\nu_{k+1|k} = 3 + d + (\alpha_{k|k} - 2)e^{-\frac{T}{\tau}} \tag{62}$$

which is equivalent to

$$\frac{1}{\alpha_{k+1|k} - 2} = \frac{e^{-\frac{T}{\tau}}}{\alpha_{k|k} - 2} \tag{63}$$

where τ is a design parameter. An alternative heuristic is given in the dissertation [8]

$$\nu_{k|k} = 3 + d + \frac{\alpha_{k|k} - 2}{1 + \left(\frac{T}{\tau}\right)\left(\alpha_{k+1|k} - 2\right)} \tag{64}$$

which is equivalent to the linear increase:

$$\frac{1}{\alpha_{k+1|k} - 2} = \frac{T}{\tau} + \frac{1}{\alpha_{k|k} - 2}. \tag{65}$$

Either of those heuristics can be used to increase the uncertainty in the target extent over time.

D. Summary of the Filter

The measurement-update step of the Bayesian extended target-tracking filter is summarized in Fig. 2. The state propagation procedure is summarized in (3). However, note that the estimation of $\tilde{\mathbf{X}}_{k|k-1}$ includes the effects of the target measurement error $\mathbf{R}_k$ if $\tilde{\mathbf{X}}_{k|k-1}$ is really representing *apparent* target extent as effected by measurement noise. This means that the addition of $\mathbf{R}_k$ in the expression for $\tilde{\mathbf{R}}_k$ is not entirely necessary. However, in practice, if one wishes to eliminate $\mathbf{R}_k$ in the expression for $\tilde{\mathbf{R}}_k$, then the diagonal elements of $\tilde{\mathbf{R}}_k$ should be adjusted so that they are never smaller than those of $\mathbf{R}_k$. In the simulations in this memo, we simply use the algorithms as written in Figs. 2 and 3.

V. Filter Initialization

To use the filter, one must be able to initialize it. The literature does not appear to describe heuristics for initialization. In this section, we suggest a heuristic.

The simplest target-initiation heuristic for the extent is:

$$\tilde{\mathbf{X}}_{0|0} = \frac{1}{z_d}\sum_{i=1}^{n_0}\left(\mathbf{z}_i^0 - \bar{\mathbf{z}}_0\right)\left(\mathbf{z}_i^0 - \bar{\mathbf{z}}_0\right)^T \qquad \nu_{0|0} = n_0 + d \qquad \bar{\mathbf{z}}_0 = \frac{1}{n_0}\sum_{i=1}^{n_0}\mathbf{z}_i^0 \tag{66}$$

because this distribution means that

$$z_d\,\mathrm{E}\left\{\mathbf{X}_0\right\} = \frac{1}{n_0 - 1}\sum_{i=1}^{n_0}\left(\mathbf{z}_i^0 - \bar{\mathbf{z}}_0\right)\left(\mathbf{z}_i^0 - \bar{\mathbf{z}}\right)^T \tag{67}$$

which is a known-unbiased covariance estimator.

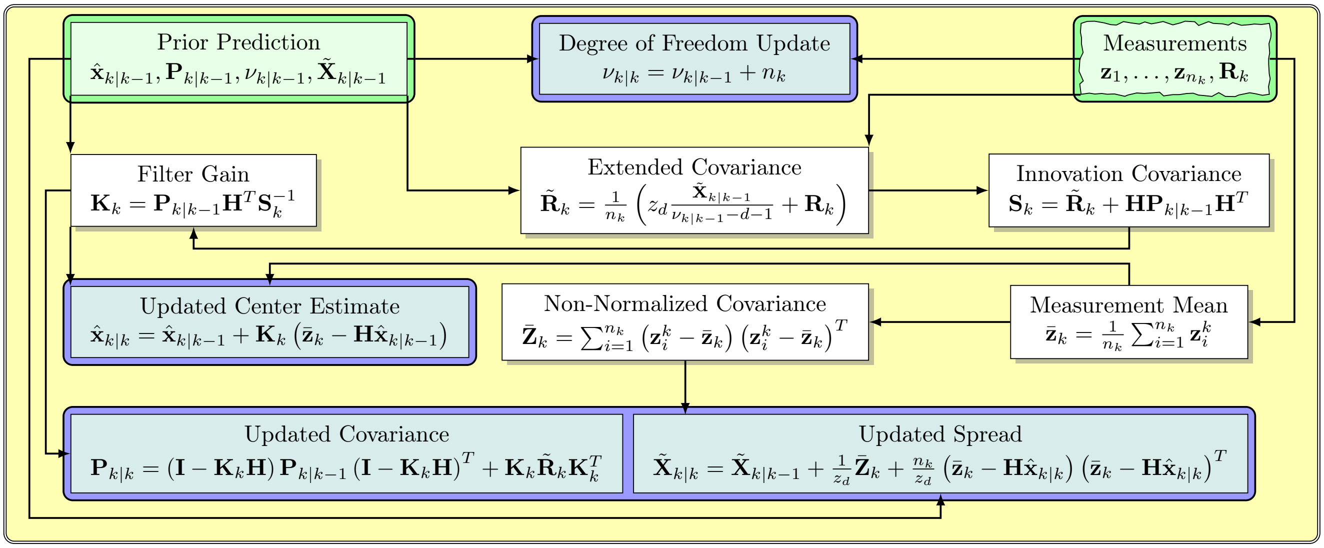

Fig. 2. The measurement-update step of the ellipsoidal extended target tracker of this paper. One will typically use $z_d = \frac{1}{d+2}$.

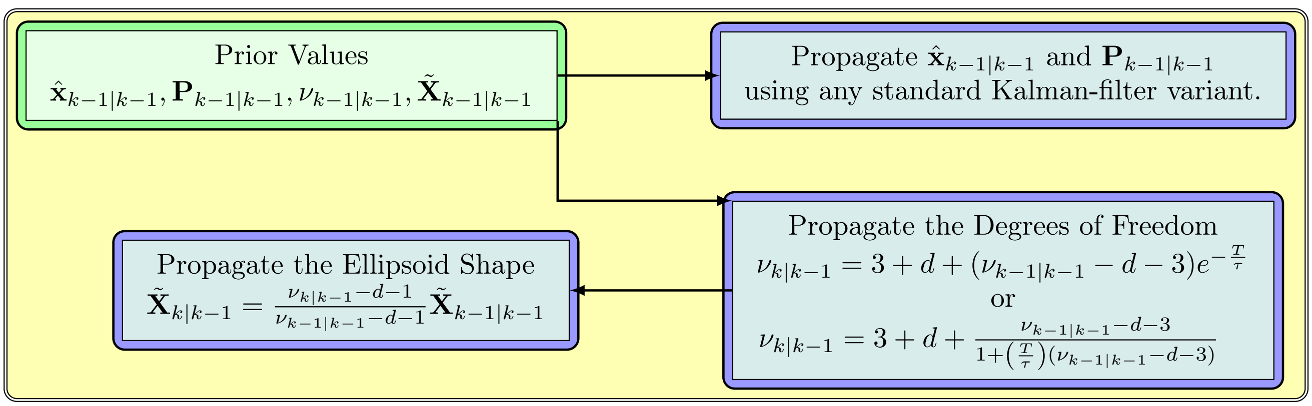

Fig. 3. The target state prediction step of the ellipsoidal extended target tracker of this paper.

For $\mathbf{x}_{0|0}$ and $\mathbf{P}_{0|0}$, one can perform single-point initiation with $\bar{\mathbf{z}}_0$ as the measurement having heuristic covariance matrix:

$$\hat{\mathbf{R}} = \texttt{clipCovMat}\left(\frac{z_d}{n_0 - 1}\tilde{\mathbf{X}}_{0|0}, \operatorname{diag}\left(\mathbf{R}\right)\right). \tag{68}$$

The heuristic "measurement" covariance matrix is the expected extent, clipped so that the diagonal elements are not less than the diagonal elements of the individual measurements. The function `clipCovMat` is in the TCL. The basic notion is that if a diagonal element of a covariance matrix exceeds a particular value, then it can be scaled. However, one cannot scale the diagonal terms in the covariance matrix independent of the off-diagonal terms (or else the result might be non-positive definite). Consequently, to scale the diagonal elements of some matrix $\mathbf{P}$ to desired values, one must multiply the covariance matrix $\mathbf{P}$ by the diagonal scaling matrix $\mathbf{S}$ in a quadratic form: $\mathbf{SPS}$. That is what the `clipCovMat` function does.

VI. Contrasting the Update with the Feldmann Method

The algorithm developed here is very similar to that presented by Feldmann, Fränken, and Koch [9]. Using the notion with $\tilde{\mathbf{X}}$ of this paper, Feldmann's algorithms differ only in the target-extent update, which is

$$\tilde{\mathbf{X}}_{k|k} = \tilde{\mathbf{X}}_{k|k-1} + \frac{1}{\alpha_{k|k-1}^2}\tilde{\boldsymbol{X}}_{k|k-1}^{\frac{1}{2}}\mathbf{S}_k^{-\frac{1}{2}}\mathbf{N}_{k|k-1}\left(\mathbf{S}_k^{-\frac{1}{2}}\right)^T\left(\tilde{\boldsymbol{X}}_{k|k-1}^{\frac{1}{2}}\right)^T + \frac{1}{\alpha_{k|k-1}^2}\tilde{\boldsymbol{X}}_{k|k-1}^{\frac{1}{2}}\tilde{\mathbf{R}}_k^{-\frac{1}{2}}\bar{\mathbf{Z}}_k\left(\tilde{\mathbf{R}}_k^{-\frac{1}{2}}\right)^T\left(\tilde{\boldsymbol{X}}_{k|k-1}^{\frac{1}{2}}\right)^T \tag{69}$$

$$\mathbf{N}_{k|k-1} \triangleq \left(\bar{\mathbf{z}}_k - \mathbf{H}\hat{\mathbf{x}}_{k|k-1}\right)\left(\bar{\mathbf{z}}_k - \mathbf{H}\hat{\mathbf{x}}_{k|k-1}\right)^T \tag{70}$$

$$\alpha_{k|k-1} = \nu_{k|k-1} - d - 1 \tag{71}$$

whereas the target-extent update presented here is

$$\tilde{\mathbf{X}}_{k|k} = \tilde{\mathbf{X}}_{k|k-1} + \frac{1}{z_d}\bar{\mathbf{Z}}_k + \frac{n_k}{z_d}\mathbf{N}_{k|k} \tag{72}$$

$$\mathbf{N}_{k|k} = \left(\bar{\mathbf{z}}_k - \mathbf{H}\hat{\mathbf{x}}_{k|k}\right)\left(\bar{\mathbf{z}}_k - \mathbf{H}\hat{\mathbf{x}}_{k|k}\right)^T. \tag{73}$$

Feldmann's derivation is an *ad-hoc* generalization of [18], [17], with modifications to obtain a rough degree of conditional unbiasedness. In Section VII, we contrast the measurement-update method of this paper with that of Feldmann and also with the measurement-update method of Orguner from [20] on a single simple example.

VII. Simulations

Though a thorough analysis of a Bayesian extended target-tracking algorithm would presumably consider a number of statistics regarding the target-ellipsoid mean and covariance matrix under different performance metrics, this memo just conveys an initial first impression, presenting an example of the performance under a single Monte Carlo run, which can be easily visualized.

We choose a scenario that is similar to the single 2D Monte Carlo run used in [9], [8]. However, whereas the measurements in [9], [8] were generated in Cartesian coordinates, we generate 2D polar measurements. The scenario involves five targets flying next to each other in formation, initially $500 -$ m apart. Range and azimuth errors are independent with standard deviations of $10\,\text{m}$ and 0.2° and the monostatic receiver is placed at the origin. A detection probability of $P_D = 0.8$ is used, though on the initialization step all five detections are obtained. The trackers are run with a discretized continuous white-noise acceleration model [1, Ch. 6.2] with power spectral density $q_0 = 70\,\text{m}^3/\text{s}^2$ (state transition matrix `FPolyKal` and covariance matrix `QPolyKal` used with the `discKalPred` function in the TCL). A measurement is obtained every $T = 10\,\text{s}$. The time constant used for the target-extent propagation is $\tau = 5\,\text{s}$. The center of the target formation moves at $300\,\text{m/s}$. Three maneuvers are performed, having accelerations of 1G, 1G, and 0.5G and then the targets spread out in the end.

We consider the approximate Bayesian measurement-update algorithm of Fig. 2 as well as the measurement update of Feldmann, which is discussed in Section VI. We also consider the measurement-update algorithm of Orguner [20], which is summarized in a flow chart in [8]. All methods used the exponential prediction step described in Fig. 3.

The true target locations during the simulation period are shown in Fig. 4a. The detections and the connected mean estimates (the red line) are shown in Fig. 4b. The approximate Bayesian mean and extent estimates are plotted in Fig. 4c with a close-up of the first turn shown in Fig. 4d. The extent and mean lines of Feldmann's algorithm and Orguner's algorithm are respectively plotted in Figs. 4e and 4f. It can be seen that the target-extent ellipses of the approximate Bayesian algorithm presented in this memo are more accurate during the second turn than those of the other algorithms. Orguner's method, being iterative, is also slower than the approximate Bayesian estimator of this paper.

VIII. Conclusion

An approximate Bayesian extended target-tracking filter was presented along with a heuristic for initializing such filters. The target's mean location is represented as a Gaussian distribution and its extent is represented in terms of an inverse-Wishart distribution. Two approximations were used to obtain decoupled measurement-update steps for the mean location and extent of the target. The performance of the filter was illustrated on a simple 2D-formation tracking example in Fig. 4, where the approximate Bayesian filter of this paper was compared with those of Feldmann [9] and Orguner [20]. On the simple example, it was observed that the approximate Bayesian tracker better estimated target-extent during maneuvers.

Future work can more thoroughly analyze the performance of the filter in comparison to alternatives. Additionally, the filter could be incorporated into an interacting multiple model filter (IMM) framework, as was done with Feldmann's filter in [9], [8]. Future work could also consider modifications to the update step such that $\tilde{\mathbf{X}}_{k|k}$ is an unbiased estimate of the target extent when $\mathbf{R}_k$ is large rather than incorporating the effects of $\mathbf{R}_k$.

Acknowledgements

This research is supported by the Office of Naval Research through the Naval Research Laboratory (NRL) Base Program.

Appendix A
Derivation of the Covariance of a Uniform Ellipsoid

We shall compute the covariance matrix of the uniform ellipsoidal PDF in (25). First, we note that when considering an integral over a scalar or vector function f with bijective transformation $\mathbf{y} = \mathbf{h}(\mathbf{x})$, the Change of Variables Theorem from multivariate calculus is

$$\int_{\mathbf{x}\in\mathbb{S}_x} f(\mathbf{x})d\mathbf{x} = \int_{\mathbf{y}\in\mathbb{S}_y} f\left(\mathbf{h}(\mathbf{y})\right)|\mathbf{J}(\mathbf{y})|d\mathbf{y} \tag{74}$$

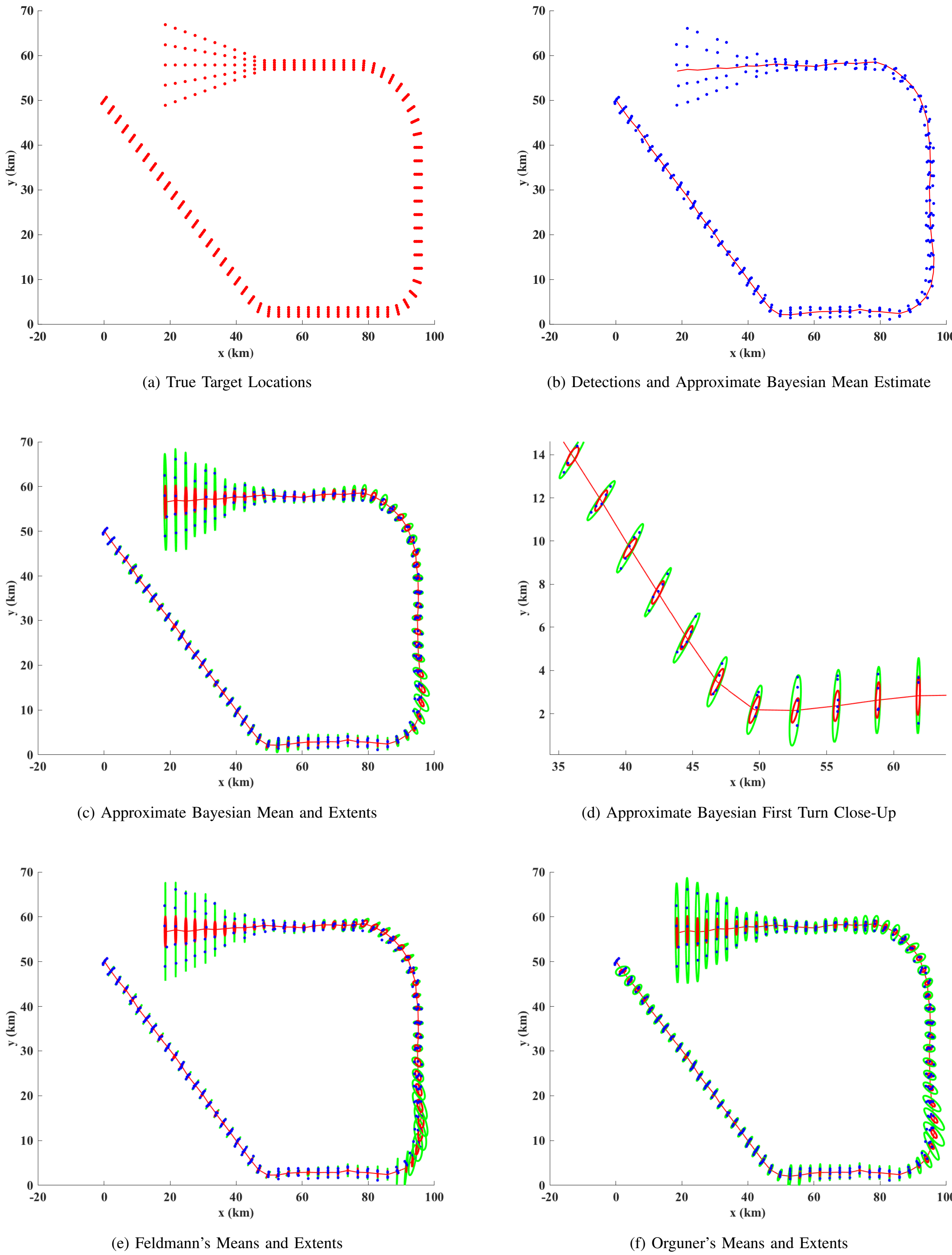

Fig. 4. Plots relating to the single Monte Carlo example of Section VII.

where $\mathbb{S}_x$ and $\mathbb{S}_y$ are the same regions but in different coordinate systems and $\mathbf{J}$ is the Jacobian matrix related to the transfromation.:

$$\mathbf{J}(\mathbf{y}) = \left[\frac{\partial}{\partial y_1} f(\mathbf{y}), \frac{\partial}{\partial y_2} f(\mathbf{y}), \ldots, \frac{\partial}{\partial y_{d_y}} f(\mathbf{y})\right] \tag{75}$$

where y is d_y-dimensional.

Without a loss of generality, we assume that $\mathbf{p}_0 = \mathbf{0}$. The covariance matrix can thus be written as

$$\mathrm{E}\left\{\mathbf{p}\mathbf{p}^T\right\} = \frac{\Gamma(\frac{d}{2}+1)}{|\mathbf{\Sigma}|^{\frac{1}{2}}\,\pi^{\frac{d}{2}}} \int\limits_{\mathbf{p}^T\mathbf{\Sigma}\mathbf{p}\leq 1} \mathbf{p}\mathbf{p}^T\, d\mathbf{p}. \tag{76}$$

Define the lower-triangular matrix $\mathbf{C}$ such that

$$\mathbf{\Sigma} \triangleq \mathbf{C}\mathbf{C}^T. \tag{77}$$

In other words, $\mathbf{C}$ is a lower-triangular Cholesky decomposition of $\mathbf{\Sigma}$. We wish to perform the change of variables that

$$\mathbf{v} = \mathbf{C}^{-1}\mathbf{p}. \tag{78}$$

Consequently, noting the relation of determinants that $|\mathbf{\Sigma}|^{\frac{1}{2}} = |\mathbf{C}|$, the Jacobian is:

$$|\mathbf{J}\left(\mathbf{v}\right)| = |\mathbf{C}|\,. \tag{79}$$

Using the Change of Variables Theorem of (74), the covariance matrix of the uniform distribution on an ellipsoid is thus:

$$\mathrm{E}\left\{\mathbf{p}\mathbf{p}^T\right\} = \frac{\Gamma(\frac{d}{2}+1)}{\pi^{\frac{d}{2}}}\mathbf{C}\left(\int\limits_{\mathbf{v}^T\mathbf{v}\leq 1} \mathbf{v}\mathbf{v}^T\, d\mathbf{v}\right)\mathbf{C}^T. \tag{80}$$

An explicit solution to the multivariate integral in (80)can be obtained from the generalized identity for $w > -d$ in [22, Ch. 7.4] that

$$\int\limits_{\mathbf{x}^T\mathbf{x}\leq 1} \left(\sum_{i=1}^{d} x_i^2\right)^{\frac{w}{2}} \left(\prod_{i=1}^{d} x_i^{\alpha_i}\right) d\mathbf{x} = \begin{cases} \left(\dfrac{2}{d+w+\sum_{i=1}^{d}\alpha_i}\right)\dfrac{\prod_{i=1}^{d}\Gamma\left(\frac{\alpha_i+1}{2}\right)}{\Gamma\left(\frac{d+\sum_{i=1}^{d}\alpha_i}{2}\right)} & \text{If all } \alpha_i \text{ are even.} \\ 0 & \text{Otherwise.} \end{cases} \tag{81}$$

Applying the formula to the problem at hand means that $w = 0$ and there either are two is such that $\alpha_i = 1$ or one such that $\alpha_i = 2$. The final expression for the covariance matrix of a uniform distribution over a d-dimensional ellipsoid is thus as given in (26).

This derivation differs slightly from [10] in that the solution is proven for all dimensions d rather than just given for $d = 1, 2, 3$.

References

[1] Y. Bar-Shalom, X. R. Li, and T. Kirubarajan, *Estimation with Applications to Tracking and Navigation: Theory, Algorithms and Software*. New York: John Wiley and Sons, 2001.

[2] Y. Bar-Shalom, P. K. Willett, and X. Tian, *Tracking and Data Fusion*. Storrs, CT: YBS Publishing, 2011.

[3] S. Blackman and R. Popoli, *Design and Analysis of Modern Tracking Systems*. Boston: Artech House, 1999.

[4] D. F. Crouse, "Basic tracking in 3D using monostatic and bistatic measurements," *IEEE Aerospace and Electronic Systems Magazine*, vol. 29, no. 8, pp. 4–53, Aug. 2014.

[5] ——, "The tracker component library: Free routines for rapid prototyping," *IEEE Aerospace and Electronic Systems*, vol. 32, no. 5, pp. 18–27, May 2017.

[6] M. H. DeGroot, *Optimal Statistical Decisions*. New York: McGraw-Hill Book Company, 1970.

[7] O. E. Drummond, S. S. Blackman, and G. C. Petrisor, "Tracking clusters and extended targets with multiple sensors," in *Technical Symposium on Optics, Electro-Optics and Sensors: Signal and Data processing of Small targets*, vol. 1305, Orlando, FL, 16-20 Apr. 1990, pp. 362–375.

[8] M. Feldmann, "Tracking von objektgruppen und ausgedehnten zielobjekten," Ph.D. dissertation, KIT-Fakultät für Informatik des Karlsruher Institut für Technologie, Karlsruhe, Germany, 30 Nov. 2018.

[9] M. Feldmann, D. Fränken, and W. Koch, "Tracking of extended objects and group targets using random matrices," *IEEE Transactions on Signal Processing*, vol. 59, no. 4, pp. 1409–1420, Apr. 2011.

[10] M. Feldmann and W. Koch, "Comments on 'Bayesian approach to extended object and cluster tracking using random matrices'," *IEEE Transactions on Aerospace and Electronic Systems*, vol. 48, no. 2, pp. 1687–1693, Apr. 2012.

[11] G. Frenkel and B. E. Fridling, "Survey of strategic defense initiative tracking algorithms," Institute for Defense Analyses, Alexandria, VA, Tech. Rep. P-2284, Nov. 1989.

[12] W.-D. Geng, Y.-Q. Wang, and Z.-H. Dong, *Group-Target Tracking*. Singapore: Springer, 2017, translated from Chinese by G. Geng and F. Yang.

[13] K. Granström, M. Baum, and S. Reuter, "Extended object tracking: Introduction, overview, and applications," *Journal of Advances in Information Fusion*, vol. 12, no. 2, pp. 139–174, Dec. 2017.

[14] K. Granström, A. Natale, P. Braca, G. Ludeno, and F. Serafino, "Gamma Gaussian inverse Wishart probability hypothesis density for extended target tracking using X-band marine radar data," *IEEE Transactions on Geoscience and Remote Sensing*, vol. 53, no. 12, pp. 6617–6631, Dec. 2015.

[15] A. K. Gupta and D. K. Nagar, *Matrix Variate Distributions*. Boca Raton: Chapman & Hall/CRC, 2000.

[16] D. G. Kabe, "A note on the Bartlett decomposition of a Wishart matrix," *Journal of the Royal Society. Seried B (Methodological)*, vol. 26, no. 2, pp. 270–273, 1964.
[17] J. W. Koch, "Bayesian approach to extended object and cluster tracking using random matrices," *IEEE Transactions on Aerospace and Electronic Systems*, vol. 44, no. 3, pp. 1042–1059, Jul. 2008.
[18] W. Koch and R. Saul, "A Bayesian approach to extended object tracking and tracking of loosely structures target groups," in *Proceedings of the 7th International Conference on Information Fusion*, Philadelphia, PA, 25–28 Jul. 2005, pp. 827–834.
[19] A. M. Kshirsagar, "Bartlett decomposition and Wishart distribution," *The Annals of Mathematical Statistics*, vol. 30, no. 1, pp. 239–241, Mar. 1959.
[20] U. Orguner, "A variational measurement update for extended target tracking with random matrices," *IEEE Transactions on Signal Processing*, vol. 60, no. 7, pp. 3827–3834, Jul. 2012.
[21] M. Polat and M. Demirekler, "Tracking of subsequently fired projectiles," in *Proceedings of the 21st Signal Processing and Communications Applications Conference*, Haspolat, Turkey, 2013, in Turkish.
[22] A. H. Stroud, *Numerical Quadrature and Solution of Ordinary Differential Equations*. New York: Springer-Verlag, 1974.
[23] H. Sun and M. Farooq, "Note on the generation of random points uniformly distributed in hyper-ellipsoids," in *Proceedings of the Fifth International Conference on Information Fusion*, Annapolis, MD, 8–11 Jul. 2002, pp. 489–496.
[24] G. Vivone, P. Braca, K. Granström, A. Natale, and J. Chanussot, "Converted measurements Bayesian extended target tracking applied to X-band marine radar data," *Journal of Advances in Information Fusion*, vol. 12, no. 2, pp. 189–210, Dec. 2017.
[25] M. J. Waxman and O. E. Drummond, "A bibliography of cluster (group) tracking," in *Proceedings of SPIE: Signal and Data Processing of Small Targets*, vol. 5428, Orlando, FL, 25 Aug. 2004, pp. 551–560.
[26] The tracker component library. [Online]. Available: https://github.com/USNavalResearchLaboratory/TrackerComponentLibrary